2016

Identification of Homogentisate Dioxygenase as a Target for Vitamin E Biofortification in Oilseeds

Minviluz G. Stacey
University of Missouri, Columbia, staceym@missouri.edu

Rebecca E. Cahoon
University of Nebraska-Lincoln, rcahoon2@unl.edu

Hanh T. Nguyen
University of Nebraska-Lincoln, hnguyen8@unl.edu

Yaya Cui
University of Missouri, Columbia

Shirley Sato
University of Nebraska - Lincoln, ssato1@unl.edu

See next page for additional authors

Identification of Homogentisate Dioxygenase as a Target for Vitamin E Biofortification in Oilseeds[1][OPEN]

Minviluz G. Stacey*, Rebecca E. Cahoon, Hanh T. Nguyen, Yaya Cui, Shirley Sato, Cuong T. Nguyen, Nongnat Phoka[2], Kerry M. Clark, Yan Liang[3], Joe Forrester, Josef Batek, Phat Tien Do, David A. Sleper, Thomas E. Clemente, Edgar B. Cahoon, and Gary Stacey

Division of Plant Sciences (M.G.S., Y.C., C.T.N., K.M.C., Y.L., J.B., P.T.D., D.A.S., G.S.), Division of Biochemistry (G.S.), and DNA Core Facility (J.F.), University of Missouri, Columbia, Missouri 65211; and Department of Biochemistry (R.E.C., N.P., E.B.C.) and Department of Agronomy and Horticulture (H.T.N., S.S., T.E.C.), Center for Plant Science Innovation, University of Nebraska, Lincoln, Nebraska 68588

ORCID IDs: 0000-0002-3774-720X (M.G.S.); 0000-0003-3392-5766 (R.E.C.); 0000-0002-8700-9598 (C.T.N.); 0000-0002-3579-7668 (N.P.); 0000-0003-3650-852X (T.E.C.); 0000-0002-7277-1176 (E.B.C.); 0000-0001-5914-2247 (G.S.).

Soybean (*Glycine max*) is a major plant source of protein and oil and produces important secondary metabolites beneficial for human health. As a tool for gene function discovery and improvement of this important crop, a mutant population was generated using fast neutron irradiation. Visual screening of mutagenized seeds identified a mutant line, designated MO12, which produced brown seeds as opposed to the yellow seeds produced by the unmodified Williams 82 parental cultivar. Using forward genetic methods combined with comparative genome hybridization analysis, we were able to establish that deletion of the *GmHGO1* gene is the genetic basis of the brown seeded phenotype exhibited by the MO12 mutant line. *GmHGO1* encodes a homogentisate dioxygenase (HGO), which catalyzes the committed enzymatic step in homogentisate catabolism. This report describes to our knowledge the first functional characterization of a plant *HGO* gene, defects of which are linked to the human genetic disease alkaptonuria. We show that reduced homogentisate catabolism in a soybean *HGO* mutant is an effective strategy for enhancing the production of lipid-soluble antioxidants such as vitamin E, as well as tolerance to herbicides that target pathways associated with homogentisate metabolism. Furthermore, this work demonstrates the utility of fast neutron mutagenesis in identifying novel genes that contribute to soybean agronomic traits.

Vitamin E is the generic term for a group of potent lipid-soluble antioxidants called tocochromanols (Kamal-Eldin and Appelqvist, 1996). Tocochromanols contain a polar chromanol head group derived from homogentisate and a long nonpolar isoprenoid side chain. Depending on the type of isoprenoid side chain that is linked to homogentisate, tocochromanols can be classified as tocopherols, tocotrienols, or plastochromanol-8 (PC-8; Fig. 1; for review, see Hunter and Cahoon, 2007; Mène-Saffrané and DellaPenna, 2010; Kruk et al., 2014). Tocopherols and tocotrienols are formed via the condensation of homogentisate with phytyl diphosphate or geranylgeranyl diphosphate (GGDP), respectively (Collakova and DellaPenna, 2001; Savidge et al., 2002; Cahoon et al., 2003; Yang et al., 2011). Tocopherols, therefore, contain fully saturated aliphatic side chains, whereas tocotrienols contain three trans double bonds. PC-8 is formed from the condensation of homogentisate with solanesyl diphosphate and has similar unsaturated, but longer, side chains as tocotrienols (Tian et al., 2007; Sadre et al., 2010; Szymańska and Kruk, 2010). Tocopherols and tocotrienols are further classified into α, β, γ, and δ isoforms depending on the number and position of methyl substitutions on their chromanol ring (Supplemental Fig. S1; Kamal-Eldin and Appelqvist, 1996). Tocopherols and tocotrienols are essential for human and livestock nutrition, specifically α-tocopherol, and have received much attention for their demonstrated anticholesterol, anticancer, and anti-inflammation activities (Kamal-Eldin and Appelqvist, 1996; Kannappan et al., 2012; Jiang, 2014; Mathur et al., 2015). Like humans and animals, plants are also subject to various oxidative stresses and require antioxidants to neutralize free radical

[1] This work was supported by the United States Department of Agriculture (National Institute of Food and Agriculture grant no. 2015-67013-22839 to E.B.C. and G.S.) and the National Science Foundation (Plant Genome Research Project grant no. IOS-1127083 to G.S. and T.E.C.).

[2] Present address: King Mongkut's University of Technology Thonburi, Ratchaburi Campus, Bangkok 10140, Thailand.

[3] Present address: Institute of Biotechnology, Zhejiang University, Hangzhou 310058, China.

* Address correspondence to staceym@missouri.edu.

The author responsible for distribution of materials integral to the findings presented in this article in accordance with the policy described in the Instructions for Authors (www.plantphysiol.org) is: Minviluz Garcia Stacey (staceym@missouri.edu).

M.G.S., E.B.C., T.E.C., and G.S. conceived the study; M.G.S., R.E.C., H.T.N., Y.C., S.S., N.P., Y.L., J.F., J.B., and P.T.D. performed the experiments; K.M.C. and D.A.S. performed and supervised genetic crosses and field propagation; C.T.N. performed data analysis and plant phenotyping; M.G.S. wrote the manuscript with contributions from the authors; E.B.C. and G.S. assisted with final manuscript revisions.

[OPEN] Articles can be viewed without a subscription.

www.plantphysiol.org/cgi/doi/10.1104/pp.16.00941

damage. Production of homogentisate-derived metabolites is thus essential for the protection of plant cells against oxidative damage during photosynthesis, abiotic stress conditions, and seed desiccation and storage (Gruszka et al., 2008; Maeda et al., 2008; Matringe et al., 2008; Falk and Munné-Bosch, 2010; Mène-Saffrané et al., 2010; Kruk et al., 2014). Tocochromanols also provide oxidative stability to plant products, such as vegetable oils, biofuels, and biobased lubricants (Clemente and Cahoon, 2009). Moreover, plastoquinone-9, which is also derived from homogentisate and is the immediate precursor of PC-8, functions as an electron carrier during photosynthesis and in desaturation reactions involved in carotenoid production (Fig. 1; Norris et al., 1995; Kern and Renger, 2007; Lichtenthaler, 2007).

Tyr and hydroxyphenylpyruvate (HPP), the immediate precursors of homogentisate, are derived from chorismate, the final product of the Shikimate pathway. Key enzymes involved in Tyr biosynthesis in plants are tightly regulated by feedback inhibition by Tyr, thereby limiting the accumulation of HPP, the direct precursor of homogentisate (Fig. 1; Tzin and Galili, 2010; Maeda and Dudareva, 2012). Transgenic plants designed to increase homogentisate accumulation by expressing microbial enzymes that bypasses this feedback inhibition resulted in increased vitamin E production (Rippert et al., 2004; Karunanandaa et al., 2005; Zhang et al., 2013). For example, HPP can be generated directly from prephenate by the yeast prephenate dehydrogenase or from chorismate by the *Escherichia coli* bifunctional chorismate mutase/prephenate dehydrogenase (TyrA). In soybean (*Glycine max*), combining seed-specific expression of TYRA and the Arabidopsis (*Arabidopsis thaliana*) HPP dioxygenase (HPPD), which converts HPP to homogentisate, resulted in an 800-fold increase in homogentisate and approximately 3-fold increase in tocochromanol levels in seeds. Coexpression of TyrA, HPPD, and homogentisate phytyl transferase, which prenylates the accumulated homogentisate using phytyl diphosphate, further increased seed tocochromanol levels to >10-fold compared to wild-type levels (Karunanandaa et al., 2005). Likewise, seed-specific expression of *E. coli* TyrA, HPPD, and barley homogentisate geranylgeranyl transferase, for prenylation of homogentisate with GGDP, resulted in large increases in homogentisate and tocochromanol levels in Arabidopsis seeds compared to wild type (Zhang et al., 2013). These biofortification efforts concluded that a major factor impeding maximal vitamin E production in plants is the availability of homogentisate. The limited cellular homogentisate pools are attributed solely to Tyr feedback inhibition, and to date, only transgenic approaches to deregulate homogentisate production are available in plants.

Besides its utilization for tocochromanol biosynthesis, homogentisate can be catabolized to acetoacetate and fumarate for central metabolism. The committed enzymatic reaction for homogentisate catabolism is the oxidation of homogentisate to maleylacetoacetate (MAA) catalyzed by homogentisate dioxygenase (HGO; Fig. 1). MAA is isomerized by maleylacetoacetate isomerase (MAAI) to fumarylacetoacetate, which is then hydrolyzed by fumarylacetoacetate hydrolase (FAH) to fumarate and acetoacetate (Lindblad et al., 1977; Mistry et al., 2013). In *Aspergillus nidulans* and *Aspergillus fumigatus*, mutations in the *hmgA* gene, encoding the fungal HGO, resulted in increased accumulation of homogentisate and a concomitant increase in the accumulation of pyomelanin, a brown pigment formed by auto-oxidation of homogentisate (Fernández-Cañón and Peñalva, 1995; Schmaler-Ripcke et al., 2009). Genetic lesions affecting the production of a functional HGO in several bacterial species also resulted in increased pyomelanin accumulation (Rodríguez-Rojas et al., 2009). In human, mutations in the gene encoding HGO (also called *HGD* or *AKU*) are the genetic basis of a rare autosomal recessive metabolic disorder called Alkaptonuria (AKU; Zatkova, 2011; Mistry et al., 2013). Consistent with *HGO* mutations reported in fungi and bacteria, AKU patients accumulate high levels of homogentisate, leading to darkened urine and pigmentation of the sclera of the eye and other connective tissues. In plants, studies on Tyr catabolism in Arabidopsis demonstrated the presence of fully functional AtHGO, AtMAAI, and AtFAH enzymes whose concerted activity can convert homogentisate to fumarate and acetoacetate (Dixon and Edwards, 2006). However, the homogentisate catabolic pathway has received only limited study in plants. This is surprising given the importance of homogentisate in vitamin E production and the potential for homogentisate catabolism to limit cellular homogentisate pools in plants.

Soybean is an important crop grown worldwide as a source of protein, vegetable oil, and secondary metabolites, including vitamin E (Karunanandaa et al., 2005; Hartman et al., 2011). The sequenced soybean genome is large and highly duplicated (Schmutz et al., 2010) and is predicted to encode 56,044 protein-coding loci and 88,647 transcripts (http://www.phytozome.net/soybean). A major challenge in soybean, as with other crop plants, is assigning function to each these genes or at least identifying those that contribute to agronomic traits. We therefore developed a large number of soybean mutants by fast neutron irradiation, a mutagen known to induce genetic deletions and segmental duplications (Li et al., 2001; Rogers et al., 2009; Bolon et al., 2011, 2014). A major advantage of this approach is that these genetic lesions can be easily defined using array-based hybridization methods (Bruce et al., 2009; Bolon et al., 2011, 2014; Haun et al., 2011). Here, we describe the functional characterization of a plant *HGO* gene and the limitation imposed by homogentisate catabolism on cellular homogentisate pools in plants. Our results show that reduced homogentisate catabolism in a soybean *HGO* mutant is an effective strategy for enhancing the production of vitamin E, as well as tolerance to herbicides that target pathways associated with homogentisate metabolism. This report also demonstrates the utility of the developed fast neutron population as a genetic resource for identifying novel genes that contribute to soybean agronomic traits.

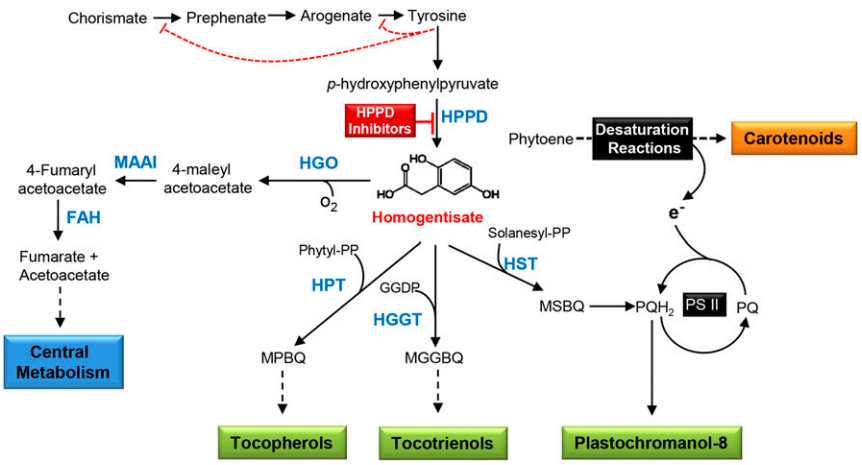

Figure 1. Diagram of homogentisate metabolic pathways in plants illustrating the importance of cellular homogentisate pools in the biosynthesis of tocochromanols and plastoquinone-9 (PQH_2), an essential electron carrier in photosynthesis and carotenoid production. Dashed arrows indicate multiple enzymatic reactions. Red dashed lines indicate feedback inhibition exerted by Tyr on key enzymes involved in homogentisate production. Chemical structures of naturally occurring tocochromanol molecules are shown in Supplemental Figure S1. HPPD inhibitors, HPPD-inhibiting herbicides; MAAI, 4-maleyl acetoacetate isomerase; FAH, 4-fumaryl acetoacetate hydrolase; HPT, homogentisate phytyl transferase; HGGT, homogentisate geranyl-geranyl transferase; HST, homogentisate solanesyl transferase; PP, diphosphate; GGDP, geranylgeranyl diphosphate; MGGBQ, 2-methyl-6-geranylgeranyl-1,4-benzoquinone; MPBQ, 2-methyl-6-phytyl-1,4-benzoquinol; MSBQ, 2-methyl-6-solanesyl-1,4-benzoquinol; PQ, plastoquinone-9; PS II, photosystem II electron transport system.

RESULTS

Genetic Lesion in *GmHGO1* Blocks Homogentisate Catabolism and Results in Increased Cellular Homogentisate Pools in Plant Cells

We developed a soybean mutant population by fast neutron irradiation of *G. max* cv Williams 82 seeds at 20, 25, 30, and 35 Gy doses. A subsequent visual screen of seeds derived from the M3 progeny of the fast neutron population identified a mutant line that produced brown seeds, as opposed to the yellow seeds produced by the wild-type Williams 82 cultivar (Fig. 2A). To characterize the genetic lesion responsible for the observed phenotype, we back-crossed the mutant line, which we designated as MO12, to the nonmodified Williams 82 cultivar and observed seeds derived from three independent crosses. We found that BC_1F_2 seeds derived from heterozygous BC_1F_1 plants were all yellow in color, similar to Williams 82 (data not shown). However, in the next generation, approximately 25% of the BC_1F_2 progeny plants produced only brown seeds, and a χ^2 test confirmed a satisfactory fit to a 3:1 ratio of yellow-seeded to brown-seeded plants (Supplemental Table S1). The brown-seeded phenotype is therefore due to a monogenic recessive genetic lesion in the MO12 genome.

In order to identify the causative gene lesion responsible for the observed phenotype, we utilized comparative genome hybridization (CGH) analysis, a microarray-based method for high-throughput identification of induced genomic deletions and additions (Bolon et al., 2011, 2014; Haun et al., 2011). CGH analysis of five brown-seeded BC_1F_2 plants detected a total of eight deleted DNA segments present in at least one of the plants analyzed (Fig. 2, B and C; Supplemental Table S2). The DNA deletions ranged from 1.4 kb to 2.6 Mb in size and encode a total of 68 predicted gene loci (Supplemental Tables S2 and S3). However, only three of these deletions are common to all of the brown-seeded plants, one in chromosome 11 and two in chromosome 12. Therefore, candidate genes responsible for the brown-seeded phenotype can be limited to the 22 predicted gene loci encoded by these overlapping deletions.

One of the gene loci within the predicted 1.7 Mb deletion on chromosome 12 (Fig. 2C) is Glyma12g20220 (designated as *GmHGO1*), which encodes an HGO enzyme involved in the conversion of homogentisate to MAA and is one of the enzymes involved in Tyr catabolism to fumarate and acetoacetate, as shown in Figure 1. Genetic defects in *HGO* are known to result in increased homogentisate accumulation in other organisms, which can give rise to a dark brown pigment when oxidized (Rodríguez-Rojas et al., 2009; Schmaler-Ripcke et al., 2009; Zatkova, 2011; Ranganath et al., 2013). We therefore hypothesized that the *GmHGO1* deletion is the causative genetic lesion responsible for the brown-seeded phenotype exhibited by the MO12 mutant. To validate the *GmHGO1* deletion predicted by CGH, we performed Southern-blot analysis using DNA from brown-seeded and yellow-seeded BC_1F_2 plants. The results confirmed the *GmHGO1* deletion predicted by CGH and, more importantly, showed cosegregation of the brown-seeded phenotype with the *GmHGO1*

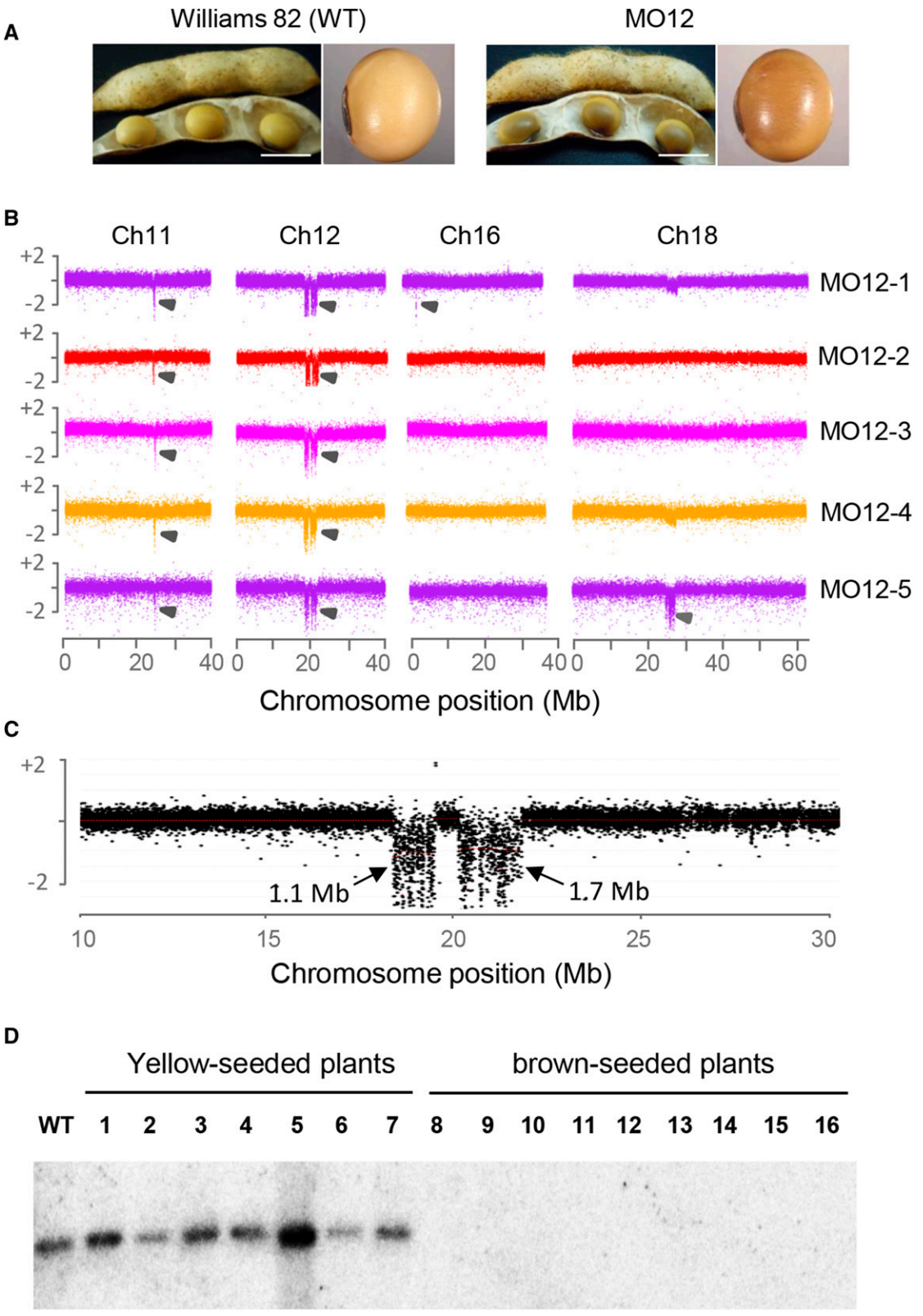

Figure 2. Seed phenotype and genetic deletions in the MO12 genome. A, Photographs of mature soybean seeds from Williams 82 (left panels) and brown-pigmented seeds from MO12 (right panels). Scale bars, 1 cm. B, Full chromosome views depicting deleted regions, indicated by arrows, detected by CGH analysis of five brown-seeded BC_1F_2 MO12 plants (MO12-1–MO12-5). C, Close-up view of Ch. 12 region containing the two deleted DNA segments common to brown-seeded BC_1F_2 plants. The 1.7 Mb

deletion (Fig. 2D). To determine if the *GmHGO1* deletion leads to a similar increase in homogentisate accumulation reported in other organisms, we performed chemical analysis of various tissues derived from MO12 and Williams 82 plants (Fig. 3A). We found that brown-colored seeds derived from homozygous *GmHGO1* deletion mutants accumulated approximately 30-fold higher homogentisate than wild-type seeds. In addition to mature seeds, homogentisate levels in leaf tissues and immature green seeds of MO12 were also significantly higher than that of Williams 82, with as much as 124-fold increase in homogentisate levels in developing seeds (Fig. 3A). In contrast, no significant differences in homogentisate accumulation in stem and root tissues of MO12 and Williams 82 plants were observed. The two deletions on chromosome 12 (Fig. 2C) are located in a low-recombination heterochromatic region and are therefore expected to cosegregate (Schmutz et al., 2010). In order to confirm that the MO12 phenotype was solely due to the deletion of *GmHGO1* rather than to codeleted gene(s) in chromosome 12, transgenic MO12 plants were generated expressing the wild-type *GmHGO1* gene expressed from its native promoter (diagrammed in Supplemental Fig. S2A). Southern-blot analysis of transgenic plants confirmed the presence of the transgene (Supplemental Fig. S2B). The complemented T_0 MO12 transgenic plants produced yellow seeds similar to the wild type (Fig. 3B) and also showed reduced levels of homogentisate in both seeds and leaves (Fig. 3, C and D). These complementation data, therefore, clearly indicate that the loss of *GmHGO1* alone is the genetic basis for the increased seed pigmentation and homogentisate accumulation in MO12 tissues. To extend this novel finding to other plant species, we obtained an Arabidopsis mutant (Salk_027807) harboring a T-DNA insertion in the *AtHGO* gene (At5g54080). Genotyping by PCR methods confirmed the T-DNA insertion in the eighth intron of *AtHGO* (Fig. 4A) and semiquantitative real-time PCR (RT-PCR) showed that the T-DNA insertion disrupted the formation of a full-length *AtHGO* transcript (Fig. 4B). Subsequent measurements of homogentisate accumulation in seeds of plants homozygous for the T-DNA insertion (*hgo1-1* allele) showed significantly higher levels of homogentisate compared to wild type (ecotype Col-0; Fig. 4C).

Taken together, these data indicate that blocking the homogentisate catabolic pathway through genetic lesions in *HGO* leads to significantly increased homogentisate accumulation in all organisms so far studied, including humans and plants.

The increased seed pigmentation in MO12 seeds, definitively shown to be due to *GmHGO1* mutation by our complementation data, is consistent with the reported increased pyomelanin production in *HGO* mutants in other organisms. Visible spectral absorption analysis offers a quick and easy procedure to detect the presence of pyomelanin in biological samples. For example, spectral absorption analysis of alkalinized homogentisate, synthetic pyomelanin, and urine samples of alkaptonuria patients showed a characteristic absorbance peak at 406 nm and 430 nm (Tokuhara et al., 2014; Roberts et al., 2015). Likewise, increased absorbance at 400 to 405 nm due to extracellular pyomelanin production was also reported in microbial *HGO* mutants (Turick et al., 2008; Schmaler-Ripcke et al., 2009; Wang et al., 2015). Spectrophotometric scan of the brown pigment extracted from MO12 seed coats showed a small peak at 400 to 405 nm and an overall higher absorbance under visible light compared to Williams 82 samples (Supplemental Fig. S3). Upon alkalinization, both Williams 82 and MO12 extracts showed significantly increased absorbance at 350 to 450 nm, but neither showed the characteristic absorbance peaks for pyomelanin. Given the relatively intense pigmentation of MO12 seeds compared to wild type, the absence of pronounced peaks associated with pyomelanin is unexpected. Pyomelanin pigment can consist of complex, heterogeneous polymers containing multiple quinone and phenolic structures, and the actual chemical nature of homogentisate-derived pigments produced by various organisms are still unknown (Roberts et al., 2015; Vasanthakumar et al., 2015). It is possible that the chemical nature of homogentisate oxidation/polymerization reactions in soybean seeds is quite different to that in other organisms and/or that chemical compounds present in MO12 seed coat extracts masked the presence of pyomelanin in our absorbance assays. Therefore, although we detected high amounts of the pyomelanin monomeric precursor (i.e. homogentisate), detailed chemical characterization of the brown pigment in MO12 seeds is needed to conclusively identify it as pyomelanin.

GmHGO1 Is the Major Isoform Expressed in Developing Soybean Seeds

Consistent with the highly duplicated nature of the soybean genome, two additional *GmHGO* loci were identified, namely Glyma06g34940 (*GmHGO2*) and Glyma06g34890 (*GmHGO3*). GmHGO1 and GmHGO2 share 92.5% amino acid identity, whereas GmHGO3

Figure 2. (*Continued.*)
deletion encodes *GmHGO1*. *y* axis in B and C represents normalized log2 ratios of MO12 to Williams 82 hybridization signals. Average and SD of normalized log2 ratios for each array was computed, and segment threshold for deletions or duplications was set at 3 SD from the array average. A complete list of deletions detected by CGH in the MO12 genome is shown in Supplemental Table S2. D, Southern blots of *Hin*dIII-restricted chromosomal DNA probed with *GmHGO1*-specific sequences. Lane WT, chromosomal DNA from Williams 82; lanes 1 to 7, chromosomal DNA from yellow-seeded BC_1F_2 MO12 plants; lanes 8 to 16, chromosomal DNA from brown-seeded BC_1F_2 MO12 plants.

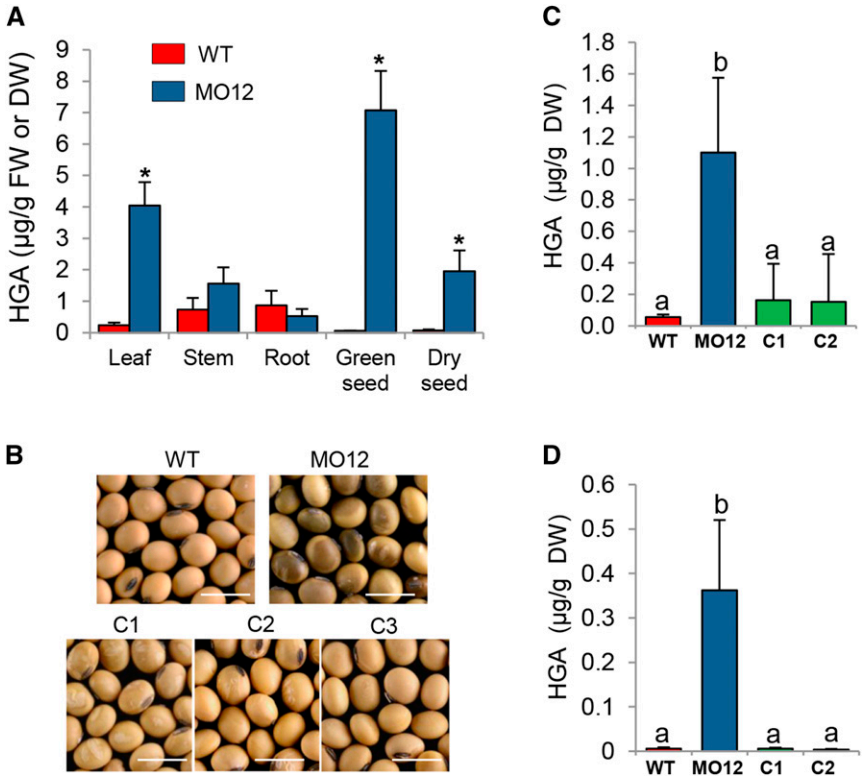

Figure 3. *GmHGO1* deletion causes increased homogentisate accumulation in soybean tissues. A, Homogentisate (HGA) levels in various tissues of Williams 82 (WT) and MO12 plants. Values represent means of 12 replicates for MO12 dry seeds and three replicates for other tissues. B, Photographs of seeds derived from Williams 82 (WT), MO12, and complemented T0 MO12 plants. C1, C2, and C3 are independent transformation events with a transgene encoding *GmHGO1* (diagrammed in Supplemental Fig. S2). Scale bars, 1 cm. C and D, Homogentisate levels in seeds (C) and leaves (D) of Williams 82 (WT), MO12, and complemented MO12 plants. Values in C and D represent means of three biological replicates for Williams 82 and MO12 and six to 15 biological replicates for C1 and C2 complemented lines. Error bars represent SD. Asterisks in A and different letters in C and D indicate significant differences between genotypes at $P < 0.01$.

showed C- and N-terminal truncations and is likely nonfunctional (Supplemental Fig. S4). Since data from our genetic and biochemical analyses showed that *GmHGO1* deletion is sufficient to cause homogentisate accumulation in seeds and leaf tissues, we investigated if this apparent lack of functional redundancy among the GmHGOs could be due to their differential expression patterns. We performed quantitative RT-PCR (qRT-PCR) on developing seeds, leaves, and roots of MO12 and Williams 82 plants and compared the expression levels of the three *GmHGO* genes in these tissues. We found that *GmHGO1* is indeed the predominant *GmHGO* gene expressed in seeds and leaves (Fig. 5A). The committed step in homogentisate catabolism in these tissues is therefore primarily catalyzed by GmHGO1, which is consistent with the significantly increased homogentisate levels in these tissues in the GmHGO1-deficient MO12 mutant compared to Williams 82 (Fig. 3A). In contrast, we found that *GmHGO1* and *GmHGO2* have comparable levels of expression in roots (Fig. 5A). The wild-type levels of homogentisate accumulation in MO12 roots (Fig. 3A) is likely due to compensating GmHGO2 activity in the mutant. *GmHGO3* expression was not detected in the tissues analyzed (data not shown), which, coupled with the predicted N- and C-terminal truncations in GmHGO3, indicate that it is likely a pseudogene. We also did not detect *GmHGO1* expression in brown-seeded MO12 tissues, consistent with the deletion of *GmHGO1* in this mutant line (Fig. 5A). These expression data are consistent with previously published genome-wide RNA-sequencing (RNA-seq) data showing higher expression of *GmHGO1* in developing soybean seeds compared to other tissues and that *GmHGO1* is expressed several-fold higher in developing seeds compared to *GmHGO2* (Libault et al., 2010; Severin et al., 2010).

Sequence analysis of GmHGO1 and GmHGO2 revealed no obvious targeting peptides indicative of cytosolic localization (data not shown). A similar cytosolic localization was also predicted for the Arabidopsis homogentisate catabolic enzymes AtHGO, AtMAAI, and AtFAH (Dixon and Edwards, 2006). In order to confirm these in silico predictions, we fused the C terminus of GmHGO1 to GFP and transiently expressed the fusion protein from a 35S promoter in tobacco leaves. A diagram of the transgene and detection of the GmHGO1-GFP fusion by western-blot analysis are shown in Supplemental Figure S5. Confocal microscopy to visualize GFP expression in infiltrated tissues showed that GmHGO1 is expressed in the cytosol (Fig. 5B). Since no free GFP was detected in the western blot (Supplemental Fig. S5), the cytosolic GFP signal is solely due to the fusion protein. These data, therefore, indicate that homogentisate catabolism indeed occurs in the cytoplasm of plant cells.

Increased Cellular Homogentisate Pools Due to GmHGO1 Deficiency Results in Increased Vitamin E Production and Tolerance to *p*-HPP Dioxygenase-Inhibiting Herbicides

In order to determine if increased cellular accumulation of homogentisate in MO12 leads to increased vitamin E production, we quantified the amounts of α, β, γ, and δ isoforms of tocopherols and tocotrienols

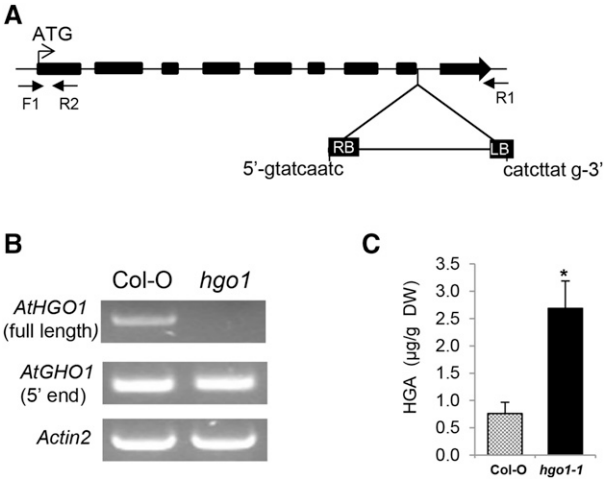

Figure 4. Isolation of Arabidopsis *AtHGO1* mutant (*hgo1-1*) and increased homogentisate (HGA) accumulation in *hgo1-1* seeds. A, Diagram of the T-DNA insertion site in *AtHGO1* (At5g54080). Boxes represent exons, and lines represent introns. RB and LB are T-DNA right and left borders, respectively. Sequences immediately flanking the T-DNA insertion are shown. B, Determination of *AtHGO1* expression in leaf tissues of Col-0 and *hgo1-1* plants by semiquantitative RT-PCR. The location of primers used to amplify full-length (primers F1 and R1) and truncated (primers F1 and R2) *AtHGO1* transcripts are indicated by arrows in A. The level of *Actin2* was used as internal control to normalize amounts of cDNA template. Primer sequences are shown in Supplemental Table S4. C, Homogentisate levels in seeds of Arabidopsis wild-type (ecotype Col-0) and *AtHGO* T-DNA insertion mutant (*hgo1-1*). Values represent means of three replicates, and error bars represent SD. Asterisk in C indicates significant difference between genotypes at $P < 0.01$.

(chemical structures are shown in Supplemental Fig. S1) in Williams 82 and MO12 seeds. Levels of γ/β-tocopherol and α-tocopherol were increased by two- and 4-fold, respectively, in MO12 seeds compared to Williams 82, whereas δ-tocopherol levels remained unchanged (Fig. 6A). Unlike tocopherols, soybean seeds normally produce negligible amounts of tocotrienols (Karunanandaa et al., 2005), which is consistent with the very low levels of tocotrienols detected in Williams 82 seeds (Fig. 6B). However, mutant seeds produced higher amounts of δ-, γ/β- and α-tocotrienol, and total tocotrienols accumulated in MO12 seeds is 27-fold higher than Williams 82. Overall, total vitamin E production in MO12 seeds was increased by approximately two-fold. Therefore, increased accumulation of homogentisate in the MO12 mutant can increase vitamin E production. These results are consistent with previous reports that homogentisate availability limits tocochromanol biosynthesis (Rippert et al., 2004; Karunanandaa et al., 2005; Zhang et al., 2013). More importantly, the data show that suppression of homogentisate catabolism via *GmHGO1* genetic lesion is a novel approach for overcoming the limitation imposed by homogentisate availability on vitamin E production in plants.

A new class of herbicides that inhibits *p*-HPPD, called HPPD inhibitors, interferes with the production of homogentisate by acting as a molecular mimic of the HPP substrate (Mitchell et al., 2001). Diminished homogentisate production upon herbicide treatment causes depletion of plastoquinone-9 and carotenoids, leading to bleaching of young foliar tissues and eventual plant death (Fig. 1; Supplemental Fig. S6A; Matringe et al., 2005). We therefore tested if the increased homogentisate accumulation in the MO12 mutant could result in increased tolerance to HPPD inhibitors. Callisto (Syngenta Crop Protection), Impact (IMVAC), or Laudis (Bayer CropScience) herbicides were painted on unifoliate soybean leaves at the vegetative stage 1 (stage V1) of development. Herbicidal activities were evaluated 15 d after herbicide application. We found that MO12 plants were indeed more tolerant to Callisto, as indicated by less foliar death of these plants compared to Williams 82 at all the herbicide concentrations tested (Fig. 7). Increased herbicidal tolerance of the MO12 mutant compared to Williams 82 was also observed for Impact (Supplemental Fig. S6B) and Laudis (data not shown). These data therefore demonstrate that, in addition increased vitamin E

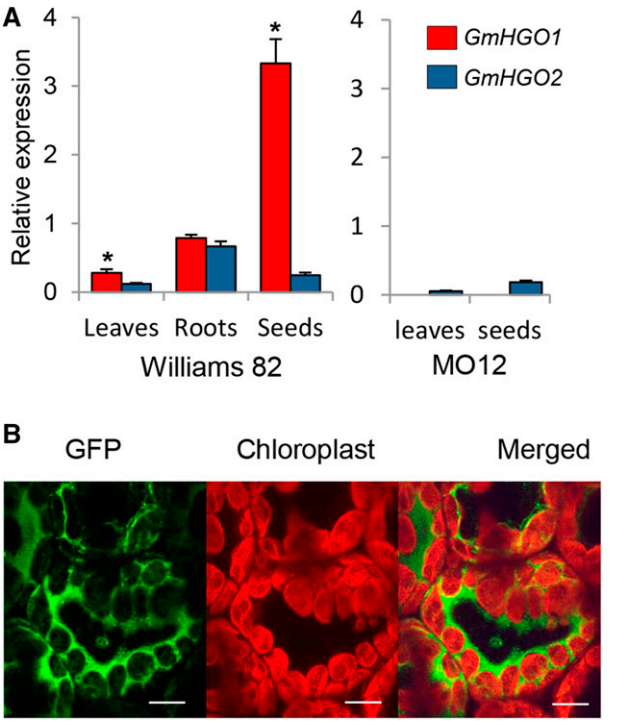

Figure 5. Expression profile of *GmHGO* genes and subcellular localization of GmHGO1. A, Expression levels of *GmHGO1* and *GmHGO2* in Williams 82 (left) and MO12 (right) tissues. Gene expression was determined by qRT-PCR on three biological samples and three technical replicates per sample. The error bars represent SD. B, Confocal images showing localization of GmHGO1-GFP (left), chloroplasts (middle), and merged image of GFP and chloroplasts (right) in *N. benthamiana* leaves. Scale bars represent 10 μm. Western-blot analysis showing GmHGO1-GFP expression in infiltrated tissues is shown in Supplemental Figure S4. Asterisks in A indicate significant differences in gene expression at $P < 0.01$.

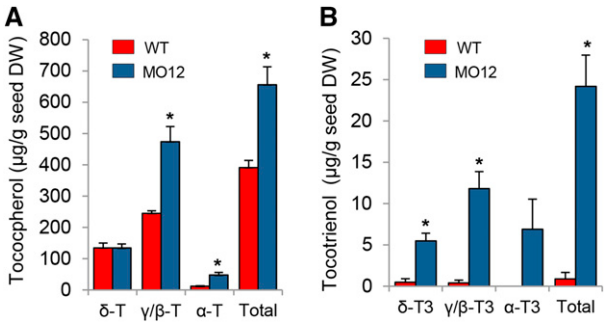

Figure 6. *GmHGO1* deletion causes increased production of vitamin E in soybean seeds. A and B, Levels of tocopherol (A) and tocotrienol (B) in Williams 82 (WT) and MO12 seeds. T, tocopherol; T3, tocotrienol; α, β, γ, and δ are naturally occurring isoforms of tocopherols and tocotrienols; γ/β, combined levels of γ and beta isoforms which were not resolved by the HPLC method employed. Values represent means of three biological replicates for Williams 82 and eight biological replicates for MO12. Error bars represent SD. Asterisks indicate significant differences between genotypes at $P < 0.01$.

production, reduced homogentisate catabolism through GmHGO1 deficiency is a viable strategy for increased tolerance to HPPD-inhibiting herbicides as well.

DISCUSSION

The soybean genome is large (~1.1 Gb) with nearly 75% of the genes present in multiple copies. Moreover, 57% of the genome is comprised of repeat-rich heterochromatic regions. (Schmutz et al., 2010). Given these features of the soybean genome, we selected fast neutron mutagenesis, a mutagen known to induce genetic deletions and segmental duplications, as a cost-effective means of obtaining genome-wide saturation mutants that can be genotyped by CGH.

Mutant plants are also nontransgenic, facilitating field propagation and integration into existing breeding programs. To provide "proof-of-concept" on the utility of the mutant population, we employed classical forward genetic approaches to identify the causative gene for the brown-seeded phenotype associated with the MO12 mutant line. CGH analysis identified eight deleted segments encoding 68 genes in the MO12 genome (Fig. 2B; Supplemental Tables S2 and S3). We subsequently identified *GmHGO1*, encoded in the chromosome 12 deletion, as the causative gene for the observed phenotype. Consistent with the highly duplicated nature of the soybean genome, we identified three *GmHGO* copies, with *GmHGO1* the predominant isoform expressed in developing seeds. Many duplicated soybean genes show subfunctionalization as exhibited by differing tissue-specific expression (Roulin et al., 2013). However, as exemplified by the *GmHGO1* deletion, subfunctionalization of soybean genes can indeed provide the opportunity to obtain phenotypic-altered mutants. Moreover, identification of the *GmHGO1* deletion demonstrates the utility of fast neutron mutagenesis coupled with genotyping by CGH as a cost-effective and rapid approach for functional genomic studies in crop plants, especially those with large and highly duplicated genomes such as soybean.

Cellular pools of homogentisate are utilized by plants in the biosynthesis of essential secondary metabolites. Of these, the most notable ones are tocochromanols, which have vitamin E and antioxidant activities (Kamal-Eldin and Appelqvist, 1996), and plastoquinone-9, a redox cofactor required for photosynthesis and carotenoid production (Norris et al., 1995; Kern and Renger, 2007; Lichtenthaler, 2007). A homogentisate glucoside, phaseoloidin, is also produced in plant trichomes as defense against insect herbivores (Weinhold et al., 2011). In this paper, the identification of the MO12 mutant allowed us to test the hypothesis that reduced homogentisate

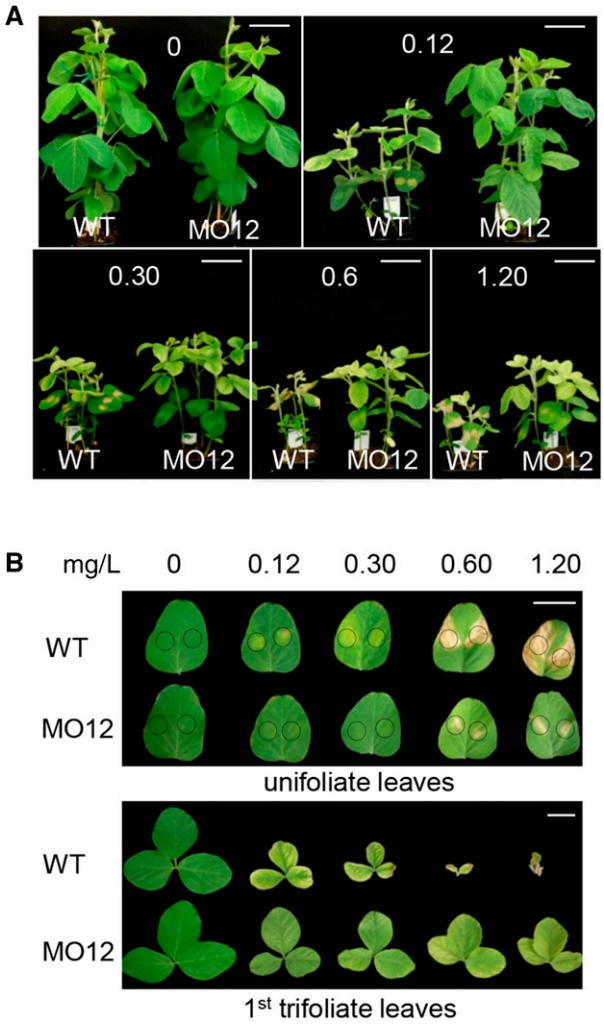

Figure 7. Increased tolerance of MO12 to *p*-HPPD-inhibiting herbicides. A, Photographs of Williams 82 (WT) and MO12 plants at 15 d after application of Callisto. Numbers are concentrations (in mg/L) of mesotrione, the active ingredient in Callisto. Scale bar, 8 cm. B, Photographs showing unifoliate and first trifoliate leaves detached from treated plants shown in B. Dashed circles indicate areas where herbicide was applied. Scale bars, 3 cm.

catabolism can effectively increase cellular homogentisate pools for enhanced production of homogentisate-derived metabolites. Indeed, seeds and leaf tissues derived from MO12 plants accumulated significantly higher homogentisate levels compared to unmodified Williams 82, with as much as 124-fold increase in homogentisate levels in developing seeds (Fig. 3A). Moreover, the deregulated accumulation of homogentisate resulted in approximately 2-fold increase in vitamin E levels in MO12 seeds (Fig. 6). In addition to tocochromanols, MO12 plants also showed increased tolerance to HPPD-inhibiting herbicides that interferes with homogentisate biosynthesis (Fig. 7; Supplemental Fig. S6). Since the herbicidal activity of HPPD inhibitors is not due to diminished homogentisate pools per se, but rather to depletion of plastoquinone-9, it is very likely that levels of this homogentisate-derived compound is increased in MO12 tissues as well. To date, limitations in homogentisate availability is attributed mainly to the tight feedback inhibition by Tyr on key enzymes involved in homogentisate biosynthesis (Tzin and Galili, 2010; Maeda and Dudareva, 2012). However, the data presented in this paper clearly show that homogentisate catabolism is also a major factor limiting the availability of homogentisate in plant cells. Moreover, reduced homogentisate catabolism through *HGO* lesions is an effective strategy for increasing homogentisate pools for the production of homogentisate-derived metabolites. The increases in seed tocochromanol concentrations achieved in the MO12 mutant are among the highest for a nontransgenic approach in an oilseed crop. Database searches indicated that *HGO* genes are present in other sequenced plant genomes, including oilseed and staple crop plants (Supplemental Table S5). Therefore, it is likely that the novel metabolic approach of enhancing cellular homogentisate pools described in this report can be applied to other plants as well. Moreover, we anticipate that transgenic expression of enzymes downstream of homogentisate would result in further increases in vitamin E levels in MO12 plants.

Tyr and 4-HPP, the immediate precursors of homogentisate, are derived from chorismate, the final product of the Shikimate pathway. The sequential reactions forming prephenate, arogenate, and Tyr, referred to as the ADH pathway (shown in Fig. 1), occur in plastids (Rippert et al., 2009; Tzin and Galili, 2010; Maeda and Dudareva, 2012). Tyr is then translocated into the cytoplasm, where it is converted to homogentisate, which is either oxidized by HGO for catabolism or translocated back into plastids for tocochromanol and plastoquinone biosynthesis (Hunter and Cahoon, 2007; Mène-Saffrané and DellaPenna, 2010; Block et al., 2013). Based on sequence analysis, cytoplasmic localization was predicted for the Arabidopsis homogentisate catabolic enzymes AtHGO, AtMAAI, and AtFAH (Dixon and Edwards, 2006). The cytoplasmic localization of GmHGO1 (Fig. 5B) supports this predicted cytoplasmic localization of homogentisate catabolism in plants. Given this scenario, reduced catabolism of homogentisate in MO12 cells would therefore increase the effective levels of homogentisate for translocation into plastids for tocochromanol production. However, it was recently reported that homogentisate can be synthesized in the plastids of soybean and likely other legumes as well (Siehl et al., 2014). This would indicate that leguminous plants can utilize plastidic homogentisate directly for secondary metabolism without necessitating transport into the plastids, as is the case in other plants. However, the increased tocochromanol production and herbicide tolerance in MO12 plants presented in this paper (Fig. 7; Supplemental Fig. S6) would imply that effective levels of cytoplasmic homogentisate for translocation into the plastids still limits the production of tocochromanols in plants, including legumes.

Relatively little data are available on the function of homogentisate, and hence Tyr, catabolism in plant growth and development. In human, deficiencies in HGO or FAH, catalyzing the last step in homogentisate catabolism, result in the genetic disease alkaptonuria (Zatkova, 2011) or tyrosinemia type I (St-Louis and Tanguay, 1997), respectively. In plants, genetic lesions in the Arabidopsis *AtFAH* gene (also called *Short-Day Sensitive Cell Death1* [*SSCD1*]) causes spontaneous cell death under short-day conditions. Cell death was attributed to the accumulation of toxic levels of MAA and FAA, as well as to their derivatives succinylacetoacetate and succinylacetone (Han et al., 2013). The cell death phenotype is reversed in plants mutated for both *AtHGO1* and *SSCD1*, confirming that the toxic metabolites are derived mainly from homogentisate catabolism induced under short day conditions. In addition to short day, increased homogentisate catabolism also occurs in senescing plant tissues as indicated by the higher expression of homogentisate catabolic genes in these tissues compared to developing tissues (Dixon and Edwards, 2006). One proposed function for homogentisate catabolism, therefore, is in the turnover of Tyr derived from the degradation of preformed protein during tissue senescence and seed germination (Dixon and Edwards, 2006). In soybean, the high *GmHGO1* expression in developing seeds (Fig. 5A) and the excessive accumulation of seed homogentisate in the *GmHGO1*mutant (Fig. 3A) clearly indicate that considerable amounts of homogentisate are catabolized during soybean seed development. A cytosolic, Tyr-insensitive pathway for Tyr production was recently identified in soybean and other legumes (Schenck et al., 2015), in addition to the plastidic pathway found in all plants shown in Figure 1. It is possible that this deregulated cytoplasmic Tyr production results in excess Tyr in developing seeds, which is catabolized through homogentisate for C and N recycling. Clearly, more work is needed to elucidate how the competing pathways for homogentisate metabolism are regulated. For example, it is curious that homogentisate catabolism appears to be induced under short day but not long day growth conditions, as indicated by the phenotypes of the Arabidopsis *sscd1* mutant mentioned above.

Transgenic approaches to express microbial and plant-derived tocochromanol biosynthetic enzymes

that bypass Tyr regulation were successful in enhancing homogentisate and tocochromanol production in plants (Rippert et al., 2004; Karunanandaa et al., 2005; Zhang et al., 2013). For example, transgenic soybean plants expressing a bacterial TYRA and the Arabidopsis HPP dioxygenase produced brown-colored seeds containing up to 800-fold more seed homogentisate relative to control (Karunanandaa et al., 2005). However, the seeds were unevenly shaped and germinated at lower rates than wild type. Similar transgenic approaches in Arabidopsis also resulted in defective seed development and germination or in reduced rosette size (Karunanandaa et al., 2005; Zhang et al., 2013). It is very likely that the high homogentisate levels attained through these transgenic approaches lead to increased accumulation of the previously mentioned toxic metabolites derived from homogentisate catabolism and hence the aberrant phenotypes. In contrast, seeds derived from the MO12 mutant are brown-colored but are otherwise normal looking (Figs. 2A and 3B) and showed no obvious germination defects (Supplemental Fig. S7A). We also found no significant differences in seed production, measured as seed weight produced per plant (Supplemental Fig. S7B), and seed size, measured as 100-seed weight (Supplemental Fig. S7C), between Williams 82 and MO12 plants. *GmHGO1* deficiency also does not appear to negatively impact storage protein and oil production in MO12 (Supplemental Fig. S7D). Lastly, field-grown Williams 82 and MO12 plants attained comparable plant height (Supplemental Fig. S7E) and number of nodes per plant (Supplemental Fig. S7F) at maturity and are indistinguishable from each other with regards to leaf development and plant architecture (data not shown). Overall, these data indicate that GmHGO1 deficiency has no significant effect on major soybean agronomic traits, at least under the normal field and greenhouse conditions we tested. However, it is possible that a functional GmHGO2 is compensating for GmHGO1 deficiency. Detailed phenotypic analysis of plants mutated for *GmHGO1* and/or *GmHGO2* is needed to verify if this is indeed the case and to further elucidate the relevance of homogentisate catabolism in soybean growth and development.

Genetically modified (GMO) crops were introduced in 1994, but a heated public debate still limits their adoption in several countries. Widely grown GMO crops either display insect or herbicide tolerance, with few engineered for improved nutritional value (Buiatti et al., 2013). The data presented in this paper demonstrate that non-GMO methods can be used to identify plant germplasm and novel strategies that can complement recombinant genetic modification approaches for crop improvement. Lastly, this work was focused on the utility of fast neutron mutagenesis in forward genetics, which remains a central component of gene function studies in plants. We do anticipate, however, that further development of this resource would expand the existing collection of fast neutron soybean mutants with known gene lesions for use in reverse genetics as well.

MATERIALS AND METHODS

Plant Material, Fast Neutron Mutagenesis, Phenotypic Screens, Genetic Crosses, and Growth Conditions

Soybean (*Glycine max*) seeds of cultivar Williams 82 were irradiated with fast neutron at 20, 25, 30, and 35 Gy doses at the McClellan Nuclear Radiation Center (University of California, Davis). Phenotypic screens for altered seed appearance (e.g. color, size, shape) were done on M_3 seeds. Back-crosses were performed by pollinating emasculated flowers of the parental cultivar Williams 82 with pollen from mutant plants grown at the Bradford Research and Experiment Center (BREC), University of Missouri, Columbia. Growth and phenotypic observations of BC_1F_2 and BC_1F_3 plants were also done on plants grown at the BREC fields in 2015. Seed increases were done at BREC and at a winter nursery in Guanacaste, Costa Rica. Soybean germination assays were done by sowing seeds on wet paper towels followed by incubation in the dark at 30°C. Seed germination was scored when the root radicle emerged from the seed coat.

The Salk_027807 Arabidopsis line harboring a T-DNA insertion in the *AtHGO* gene (At5g54080) was obtained from the Arabidopsis Biological Research Center. T-DNA insertion in *AtHGO* was confirmed by PCR and subsequent sequencing of the amplified PCR product. Primers used in PCR amplification and sequencing are listed in Supplemental Table S4. Arabidopsis plants were planted in Pro-Mix soil (Premier Horticulture) and grown at 22°C under 16-h light regime at 120 μmol m^{-2} s^{-1} fluorescent white light intensity.

CGH and Data Analyses to Identify Copy Number Variation (CNV) Events

CGH was performed using a 696,139-feature soybean CGH microarray (Bolon et al., 2011; Haun et al., 2011). The oligonucleotide probes are 50- to 70-mers spaced at approximately 1.1 kb intervals and were designed by Roche NimbleGen based on the sequenced Williams 82 genome. MO12 and Williams 82 (reference cultivar) chromosomal DNA was isolated from young leaf tissues using the Qiagen Plant DNeasy Mini Kit and labeled with cy3 and cy5, respectively. DNA labeling, hybridizations, and data analysis were performed following the manufacturer's established guidelines. For each CGH dataset, the average and SD values for corrected $\log_2$ ratios of the 696,139 unique probes were obtained. Significant CNV events were called following previously set criteria (Bolon et al., 2011), namely, segments with an average corrected $\log_2$ ratio values greater than or less than three SD from the array mean were identified as additions or deletions, respectively. Likewise, if a gap between potential segments was less than half the size of the total distance covered by neighboring segments, then the entire region was considered a single CNV event. CNV events that fall within the known heterogenic regions of the Williams 82 genome (Haun et al., 2011) were not included. CNV events in the MO12 genome were submitted in publicly available soybean databases (http://soybase.org) as part of a broader project on developing fast neutron mutant population resource for soybean.

Homogentisate Measurements and Spectral Absorption Analysis of Seed Coat Extracts

Homogentisate measurement by ESI-LC/MS/MS was carried out essentially as previously described (Zhang et al., 2013). Briefly, 100 mg of dry soybean seed or fresh weight of vegetative tissues 100 mg of was extracted in 1 mL of methanol: water (50:50) with 0.1% formic acid. Extracts were separated on an Eclipse Plus C18 column, 2.1 × 50 mm, 1.8 μM (Agilent Technologies) using a Shimadzu Prominence UPLC system operated at a flow rate of 0.2 mL/min. Homogentisate was monitored by the MRM transition 167.1/123.1 *m/z* using a QTRAP4000 triple quadrupole mass spectrometer (AB SCIEX) operated in negative mode, as described previously.

For spectral absorption analysis of seed coat extracts, 30 mg seed coats were detached from Williams 82 or MO12 seeds and ground to fine powder using mortar and pestle. Ground samples were suspended in 1 mL water, shaken for 10 min at room temperature, incubated in water bath at 37°C for 10 min and then centrifuged at 18,000*g* for 20 min. The supernatant was either alkalinized with 20 μL 5 M NaOH or amended with 20 μL distilled water for 1 min. The absorption spectra from 350 nm to 600 nm at 5 nm intervals was determined using a Synergy 2 Multi-Mode Microplate Reader (BioTek Instruments) on 200 μL aliquots with distilled water set as the blank.

Determination of Tocochromanol Content and Composition

Finely ground dry soybean seeds (30–50 mg) or freshly harvested leaf tissue (50–100 mg) were extracted in 9:1 methanol:dichloromethane containing 5000 ng (for seed analysis) or 500 ng (for leaf analysis) of 5,7-dimethyltocol (Matreya) as an internal standard. Tocochromanols were analyzed by HPLC as previously described (Zhang et al., 2013).

RNA Isolation, cDNA Synthesis, and Transcript Level Analysis

RNA extraction was performed using TRIzol reagent (Invitrogen) following the manufacturer's instructions. cDNA was synthesized using oligo(dT) primers (15-mer) and M-MLV reverse transcriptase enzyme (Promega) following the manufacturer's instructions. Transcript levels of *AtHGO1* were determined by semiquantitative RT-PCR using the Arabidopsis (*Arabidopsis thaliana*) *ACTIN2* as a control for cDNA synthesis. Transcript levels of *GmHGO* genes were determined by qRT-PCR using an ABI17500 real-time PCR following the SYBR Green method (Applied Biosystems). Gene expression levels were normalized to the expression of the soybean housekeeping genes *cons6* and *cons4* (Libault et al., 2008). Primers used for RT-PCR are listed in Supplemental Table S4.

Construction of *GmHGO1-GFP* Fusion, Transient Expression in Tobacco Leaves, Western-Blot Analysis, and Microscopy

pCambia35S-GFP was constructed by replacing the *GUS* gene encoded in pCambia 1391Z with the 35S promoter and eGFP from pEGAD. The *GmHGO1* CDS was amplified by PCR using the cDNA library described above as template. The amplified PCR product was cloned in-frame with the eGFP encoded in the pCambia35S-GFP vector. The resulting plasmid construct, pCambia*35S-GmHGO1-GFP* (diagrammed in Supplemental Fig. S5A), was transformed into *Agrobacterium tumefaciens* EHA105. *Agrobacterium*-mediated transient expression in *Nicotiana benthamiana* plants was done following routine procedures. Tissue sections from infiltrated leaf areas were viewed under a Zeiss LSM 510 META NLO two-photon-scanning confocal microscope with a 40× water objective. Total protein was extracted from infiltrated leaf areas and analyzed by western-blot hybridization using anti-GFP antibody (Miltenyl Biotec). Signals were detected by Supersignal substrate (Pierce), and Ponceau S (Sigma) staining was used as the loading control. Primer sequences for *GmHGO1* cDNA amplification are shown in Supplemental Table S4.

Southern-Blot Analysis

Chromosomal DNA was isolated from young leaf tissues following routine isolation techniques. RNAse A-treated genomic DNA was digested with *Hin*dIII or *Eco*RI and separated on a 0.8% agarose TAE Gel. A 404 bp fragment internal to the *HGO1* genomic sequence was PCR-amplified and labeled with α^{32}P-dATP (3000 Ci/mol) using the Prime-a-Gene DNA labeling system (Promega). *GmHGO1*-hybridizing bands were visualized with a FujiFilm Fluorescent Imager Analyzer FLA 3000. Primers sequences for probe amplification are listed in Supplemental Table S4.

Genetic Complementation and Soybean Transformation

The full length *GmHGO1* genomic sequence was PCR-amplified and cloned into the *Xho*I/*Bam*HI sites of the soybean binary vector pFGC5941 to give the pFGC35S-HGO1 construct. The *HGO1* promoter region (3.0 kb) was also PCR-amplified and cloned 5′ of the *HGO1* sequence in pFGC35S-HGO1 (*Eco*RI/*Xho*I sites). The resulting construct, pFGCpro2-Gm*HGO1*, was transformed into *A. tumefaciens* strain AGL1. Stable transformation of the MO12 mutant soybean line was conducted via *Agrobacterium*-mediated gene transfer using the cotyledonary-node explant method and employing glufosinate as selection agent (Zhang et al., 1999). Primer sequences for *GmHGO1* genomic DNA amplification are listed in Supplemental Table S4.

Herbicide Resistance Assays

Soybean seeds were germinated and grown in the green house until vegetative stage I (stage V1) when the unifoliate leaves were fully expanded and the emerging first trifoliate leaves were at most 1 cm long. Callisto (Syngenta Crop Protection), Impact (IMVAC), and Laudis (Bayer CropScience) herbicides were painted on unifoliate leaves using a cotton-tipped applicator. Herbicides were prepared in 1% Silwet L-77 solution at 0.12, 0.30, 0.60, and 1.20 mg/L for mesotrione (active ingredient in Callisto) and tembotrione (active ingredient in Laudis) and at 0.08, 0.20, 0.40, and 0.80 mg/L for topramezone (active ingredient in Impact). Control plants received 1% Silwet solution. Foliar death was observed 15 d after herbicide treatment.

Statistical Procedures

Sample means between genotypes or treatments were compared using t-test or one-way ANOVA followed by a post-hoc Duncan's multiple range test. All statistical analyses were performed using SAS/STAT software version 9.4.

Accession Numbers

Sequence data from this article can be found at the Phytozome, Soybase, SoyKB or the Arabidopsis Information Database: GmHGO1 (Glyma12g20220 or Glyma.12g158600), GmHGO2 (Glyma06g34940 or Glyma.06g234200), GmHGO3 (Glyma06g34890 or Glyma.06g233800), AtHGO1 (At5g54080), ACTIN 2 (At3g18780), pEGAD vector (AF218816) and pFGC5941 vector (AY310901). Additional HGO sequence data are listed in Supplemental Table S5.

Supplemental Data

The following supplemental materials are available.

Supplemental Figure S1. Chemical structures of tocotrienols and tocopherols.

Supplemental Figure S2. Construction of binary vector expressing *GmHGO1*and Southern-blot analysis of transgenic soybean plants.

Supplemental Figure S3. Absorption spectra of Williams 82 (wild type) and MO12 seed coat extracts.

Supplemental Figure S4. Full-length amino acid sequence alignment of human (HsHGO), Arabidopsis (AtHGO), and soybean HGO proteins.

Supplemental Figure S5. Construction of *GmHGO1-GFP* and detection of the fusion protein in tobacco.

Supplemental Figure S6. Increased resistance of the MO12 mutant to the HPPD herbicide Impact.

Supplemental Figure S7. Comparison of measured growth, seed yield, and seed quality between Williams 82 (wild-type) and MO12 plants.

Supplemental Table S1. Segregation of brown-seeded phenotype in BC_1F_2 plants derived from three Williams 82 × MO12 back-crosses.

Supplemental Table S2. Deleted genomic segment borders detected by CGH in at least one of the brown-seeded BC_1F_2 MO12 plants.

Supplemental Table S3. List of genes within deleted DNA segments detected by CGH on brown-seeded BC_1F_2 MO12 plants.

Supplemental Table S4. Primer sequences used to amplify various genes or identify knockout lines.

Supplemental Table S5. Hidden Markov model (http://hmmer.org/) profile search for HGO homologs/orthologs in the Phytozome database.

ACKNOWLEDGMENTS

We thank R. Stupar, W.J. Haun, Y.-T. Bolon, and C.P. Vance for technical assistance on CGH analysis (University of Minnesota); N. Gomez-Hernandez, N. Ramirez-Perez, O. Valdes, B. Frey, and A. Jurkevic for technical and field assistance, K. Bradley for providing HPPD-inhibiting herbicides, D. Mendoza-Cozatl for providing anti-GFP antibody, and the DNA Core facility for equipment support (University of Missouri); and the Arabidopsis Biological Resource Center for providing the *hgo1-1* Arabidopsis mutant.

Received June 15, 2016; accepted September 17, 2016; published September 22, 2016.

LITERATURE CITED

Block A, Fristedt R, Rogers S, Kumar J, Barnes B, Barnes J, Elowsky CG, Wamboldt Y, Mackenzie SA, Redding K, et al (2013) Functional modeling identifies paralogous solanesyl-diphosphate synthases that assemble the side chain of plastoquinone-9 in plastids. J Biol Chem **288:** 27594–27606

Bolon YT, Haun WJ, Xu WW, Grant D, Stacey MG, Nelson RT, Gerhardt DJ, Jeddeloh JA, Stacey G, Muehlbauer GJ, et al (2011) Phenotypic and genomic analyses of a fast neutron mutant population resource in soybean. Plant Physiol **156:** 240–253

Bolon YT, Stec AO, Michno JM, Roessler J, Bhaskar PB, Ries L, Dobbels AA, Campbell BW, Young NP, Anderson JE, et al (2014) Genome resilience and prevalence of segmental duplications following fast neutron irradiation of soybean. Genetics **198:** 967–981

Bruce M, Hess A, Bai J, Mauleon R, Diaz MG, Sugiyama N, Bordeos A, Wang GL, Leung H, Leach JE (2009) Detection of genomic deletions in rice using oligonucleotide microarrays. BMC Genomics **10:** 129

Buiatti M, Christou P, Pastore G (2013) The application of GMOs in agriculture and in food production for a better nutrition: two different scientific points of view. Genes Nutr **8:** 255–270

Cahoon EB, Hall SE, Ripp KG, Ganzke TS, Hitz WD, Coughlan SJ (2003) Metabolic redesign of vitamin E biosynthesis in plants for tocotrienol production and increased antioxidant content. Nat Biotechnol **21:** 1082–1087

Clemente TE, Cahoon EB (2009) Soybean oil: genetic approaches for modification of functionality and total content. Plant Physiol **151:** 1030–1040

Collakova E, DellaPenna D (2001) Isolation and functional analysis of homogentisate phytyltransferase from Synechocystis sp. PCC 6803 and Arabidopsis. Plant Physiol **127:** 1113–1124

Dixon DP, Edwards R (2006) Enzymes of tyrosine catabolism in Arabidopsis thaliana. Plant Sci **171:** 360–366

Falk J, Munné-Bosch S (2010) Tocochromanol functions in plants: antioxidation and beyond. J Exp Bot **61:** 1549–1566

Fernández-Cañón JM, Peñalva MA (1995) Molecular characterization of a gene encoding a homogentisate dioxygenase from Aspergillus nidulans and identification of its human and plant homologues. J Biol Chem **270:** 21199–21205

Gruszka J, Pawlak A, Kruk J (2008) Tocochromanols, plastoquinol, and other biological prenyllipids as singlet oxygen quenchers-determination of singlet oxygen quenching rate constants and oxidation products. Free Radic Biol Med **45:** 920–928

Han C, Ren C, Zhi T, Zhou Z, Liu Y, Chen F, Peng W, Xie D (2013) Disruption of fumarylacetoacetate hydrolase causes spontaneous cell death under short-day conditions in Arabidopsis. Plant Physiol **162:** 1956–1964

Hartman GL, West ED, Herman TK (2011) Crops that feed the World 2. Soybean-worldwide production, use, and constraints caused by pathogens and pests. Food Secur **3:** 5–17

Haun WJ, Hyten DL, Xu WW, Gerhardt DJ, Albert TJ, Richmond T, Jeddeloh JA, Jia G, Springer NM, Vance CP, et al (2011) The composition and origins of genomic variation among individuals of the soybean reference cultivar Williams 82. Plant Physiol **155:** 645–655

Hunter SC, Cahoon EB (2007) Enhancing vitamin E in oilseeds: unraveling tocopherol and tocotrienol biosynthesis. Lipids **42:** 97–108

Jiang Q (2014) Natural forms of vitamin E: metabolism, antioxidant, and anti-inflammatory activities and their role in disease prevention and therapy. Free Radic Biol Med **72:** 76–90

Kamal-Eldin A, Appelqvist LA (1996) The chemistry and antioxidant properties of tocopherols and tocotrienols. Lipids **31:** 671–701

Kannappan R, Gupta SC, Kim JH, Aggarwal BB (2012) Tocotrienols fight cancer by targeting multiple cell signaling pathways. Genes Nutr **7:** 43–52

Karunanandaa B, Qi Q, Hao M, Baszis SR, Jensen PK, Wong YH, Jiang J, Venkatramesh M, Gruys KJ, Moshiri F, et al (2005) Metabolically engineered oilseed crops with enhanced seed tocopherol. Metab Eng **7:** 384–400

Kern J, Renger G (2007) Photosystem II: structure and mechanism of the water:plastoquinone oxidoreductase. Photosynth Res **94:** 183–202

Kruk J, Szymańska R, Cela J, Munne-Bosch S (2014) Plastochromanol-8: fifty years of research. Phytochemistry **108:** 9–16

Li X, Song Y, Century K, Straight S, Ronald P, Dong X, Lassner M, Zhang Y (2001) A fast neutron deletion mutagenesis-based reverse genetics system for plants. Plant J **27:** 235–242

Libault M, Farmer A, Joshi T, Takahashi K, Langley RJ, Franklin LD, He J, Xu D, May G, Stacey G (2010) An integrated transcriptome atlas of the crop model Glycine max, and its use in comparative analyses in plants. Plant J **63:** 86–99

Libault M, Thibivilliers S, Bilgin DD, Radwan O, Benitez M, Clough SJ, Stacey G (2008) Identification of four soybean reference genes for gene expression normalization. Plant Genome **1:** 44–54

Lichtenthaler HK (2007) Biosynthesis, accumulation and emission of carotenoids, alpha-tocopherol, plastoquinone, and isoprene in leaves under high photosynthetic irradiance. Photosynth Res **92:** 163–179

Lindblad B, Lindstedt S, Steen G (1977) On the enzymic defects in hereditary tyrosinemia. Proc Natl Acad Sci USA **74:** 4641–4645

Maeda H, Dudareva N (2012) The shikimate pathway and aromatic amino acid biosynthesis in plants. Annu Rev Plant Biol **63:** 73–105

Maeda H, Sage TL, Isaac G, Welti R, Dellapenna D (2008) Tocopherols modulate extraplastidic polyunsaturated fatty acid metabolism in Arabidopsis at low temperature. Plant Cell **20:** 452–470

Mathur P, Ding Z, Saldeen T, Mehta JL (2015) Tocopherols in the prevention and treatment of atherosclerosis and related cardiovascular disease. Clin Cardiol **38:** 570–576

Matringe M, Ksas B, Rey P, Havaux M (2008) Tocotrienols, the unsaturated forms of vitamin E, can function as antioxidants and lipid protectors in tobacco leaves. Plant Physiol **147:** 764–778

Matringe M, Sailland A, Pelissier B, Rolland A, Zink O (2005) p-Hydroxyphenylpyruvate dioxygenase inhibitor-resistant plants. Pest Manag Sci **61:** 269–276

Mène-Saffrané L, DellaPenna D (2010) Biosynthesis, regulation and functions of tocochromanols in plants. Plant Physiol Biochem **48:** 301–309

Mène-Saffrané L, Jones AD, DellaPenna D (2010) Plastochromanol-8 and tocopherols are essential lipid-soluble antioxidants during seed desiccation and quiescence in Arabidopsis. Proc Natl Acad Sci USA **107:** 17815–17820

Mistry JB, Bukhari M, Taylor AM (2013) Alkaptonuria. Rare Dis **1:** e27475

Mitchell G, Bartlett DW, Fraser TE, Hawkes TR, Holt DC, Townson JK, Wichert RA (2001) Mesotrione: a new selective herbicide for use in maize. Pest Manag Sci **57:** 120–128

Norris SR, Barrette TR, DellaPenna D (1995) Genetic dissection of carotenoid synthesis in arabidopsis defines plastoquinone as an essential component of phytoene desaturation. Plant Cell **7:** 2139–2149

Ranganath LR, Jarvis JC, Gallagher JA (2013) Recent advances in management of alkaptonuria. J Clin Pathol **66:** 367–373

Rippert P, Puyaubert J, Grisollet D, Derrier L, Matringe M (2009) Tyrosine and phenylalanine are synthesized within the plastids in Arabidopsis. Plant Physiol **149:** 1251–1260

Rippert P, Scimemi C, Dubald M, Matringe M (2004) Engineering plant shikimate pathway for production of tocotrienol and improving herbicide resistance. Plant Physiol **134:** 92–100

Roberts NB, Curtis SA, Milan AM, Ranganath LR (2015) The pigment in alkaptonuria relationship to melanin and other coloured substances: a review of metabolism, composition and chemical analysis. JIMD Rep **24:** 51–66

Rodríguez-Rojas A, Mena A, Martín S, Borrell N, Oliver A, Blázquez J (2009) Inactivation of the hmgA gene of Pseudomonas aeruginosa leads to pyomelanin hyperproduction, stress resistance and increased persistence in chronic lung infection. Microbiology **155:** 1050–1057

Rogers C, Wen J, Chen R, Oldroyd G (2009) Deletion-based reverse genetics in Medicago truncatula. Plant Physiol **151:** 1077–1086

Roulin A, Auer PL, Libault M, Schlueter J, Farmer A, May G, Stacey G, Doerge RW, Jackson SA (2013) The fate of duplicated genes in a polyploid plant genome. Plant J **73:** 143–153

Sadre R, Frentzen M, Saeed M, Hawkes T (2010) Catalytic reactions of the homogentisate prenyl transferase involved in plastoquinone-9 biosynthesis. J Biol Chem **285:** 18191–18198

Savidge B, Weiss JD, Wong YH, Lassner MW, Mitsky TA, Shewmaker CK, Post-Beittenmiller D, Valentin HE (2002) Isolation and characterization of homogentisate phytyltransferase genes from Synechocystis sp. PCC 6803 and Arabidopsis. Plant Physiol **129:** 321–332

Schenck CA, Chen S, Siehl DL, Maeda HA (2015) Non-plastidic, tyrosine-insensitive prephenate dehydrogenases from legumes. Nat Chem Biol **11:** 52–57

Schmaler-Ripcke J, Sugareva V, Gebhardt P, Winkler R, Kniemeyer O, Heinekamp T, Brakhage AA (2009) Production of pyomelanin, a second

type of melanin, via the tyrosine degradation pathway in Aspergillus fumigatus. Appl Environ Microbiol **75:** 493–503

Schmutz J, Cannon SB, Schlueter J, Ma J, Mitros T, Nelson W, Hyten DL, Song Q, Thelen JJ, Cheng J, et al (2010) Genome sequence of the palaeopolyploid soybean. Nature **463:** 178–183

Severin AJ, Woody JL, Bolon YT, Joseph B, Diers BW, Farmer AD, Muehlbauer GJ, Nelson RT, Grant D, Specht JE, et al (2010) RNA-Seq atlas of Glycine max: a guide to the soybean transcriptome. BMC Plant Biol **10:** 160

Siehl DL, Tao Y, Albert H, Dong Y, Heckert M, Madrigal A, Lincoln-Cabatu B, Lu J, Fenwick T, Bermudez E, et al (2014) Broad 4-hydroxyphenylpyruvate dioxygenase inhibitor herbicide tolerance in soybean with an optimized enzyme and expression cassette. Plant Physiol **166:** 1162–1176

St-Louis M, Tanguay RM (1997) Mutations in the fumarylacetoacetate hydrolase gene causing hereditary tyrosinemia type I: overview. Hum Mutat **9:** 291–299

Szymańska R, Kruk J (2010) Plastoquinol is the main prenyllipid synthesized during acclimation to high light conditions in Arabidopsis and is converted to plastochromanol by tocopherol cyclase. Plant Cell Physiol **51:** 537–545

Tian L, DellaPenna D, Dixon RA (2007) The pds2 mutation is a lesion in the Arabidopsis homogentisate solanesyltransferase gene involved in plastoquinone biosynthesis. Planta **226:** 1067–1073

Tokuhara Y, Shukuya K, Tanaka M, Mouri M, Ohkawa R, Fujishiro M, Takahashi T, Okubo S, Yokota H, Kurano M, et al (2014) Detection of novel visible-light region absorbance peaks in the urine after alkalization in patients with alkaptonuria. PLoS One **9:** e86606

Turick CE, Caccavo F Jr, Tisa LS (2008) Pyomelanin is produced by Shewanella algae BrY and affected by exogenous iron. Can J Microbiol **54:** 334–339

Tzin V, Galili G (2010) New insights into the shikimate and aromatic amino acids biosynthesis pathways in plants. Mol Plant **3:** 956–972

Vasanthakumar A, DeAraujo A, Mazurek J, Schilling M, Mitchell R (2015) Pyomelanin production in Penicillium chrysogenum is stimulated by L-tyrosine. Microbiology **161:** 1211–1218

Wang H, Qiao Y, Chai B, Qiu C, Chen X (2015) Identification and molecular characterization of the homogentisate pathway responsible for pyomelanin production, the major melanin constituents in Aeromonas media WS. PLoS One **10:** e0120923

Weinhold A, Shaker K, Wenzler M, Schneider B, Baldwin IT (2011) Phaseoloidin, a homogentisic acid glucoside from Nicotiana attenuata trichomes, contributes to the plant's resistance against lepidopteran herbivores. J Chem Ecol **37:** 1091–1098

Yang W, Cahoon RE, Hunter SC, Zhang C, Han J, Borgschulte T, Cahoon EB (2011) Vitamin E biosynthesis: functional characterization of the monocot homogentisate geranylgeranyl transferase. Plant J **65:** 206–217

Zatkova A (2011) An update on molecular genetics of Alkaptonuria (AKU). J Inherit Metab Dis **34:** 1127–1136

Zhang C, Cahoon RE, Hunter SC, Chen M, Han J, Cahoon EB (2013) Genetic and biochemical basis for alternative routes of tocotrienol biosynthesis for enhanced vitamin E antioxidant production. Plant J **73:** 628–639

Zhang Z, Xing A, Staswick P, Clemente TE (1999) The use of glufosinate as a selective agent in Agrobacterium-mediated transformation of soybean. Plant Cell Tissue Organ Cult **56:** 37–46